Scientia Pharmaceutica

ÖSTERREICHISCHE PHARMAZEUTISCHE GESELLSCHAFT

MDPI

Article

Comparative Study of Microspicules vs. Microneedles as Potential Transdermal Delivery Systems for *Boesenbergia rotunda*-Loaded Microemulsion Formulation

Panatda Wittayanukullack [1,2], Kusuma Jitsaeng [1,3], Phaijit Sritananuwat [3,4], Charuwan Thanawiroon [1], Phuvamin Suriyaaumporn [2], Praneet Opanasopit [2,*] and Worranan Rangsimawong [1,3,*]

[1] Department of Pharmaceutical Chemistry and Technology, Faculty of Pharmaceutical Sciences, Ubon Ratchathani University, Ubon Ratchathani 34190, Thailand; panatda.p@ubu.ac.th (P.W.); kusuma.j@ubu.ac.th (K.J.); charuwan.t@ubu.ac.th (C.T.)
[2] Department of Industrial Pharmacy, Faculty of Pharmacy, Silpakorn University, Nakhon Pathom 73000, Thailand; suriyaamporn_p@su.ac.th
[3] Innovation in Drug and Extract of Agriculture Research Center, Faculty of Pharmaceutical Sciences, Ubon Ratchathani University, Ubon Ratchathani 34190, Thailand; phaijit.s@ubu.ac.th
[4] Department of Biopharmacy, Faculty of Pharmaceutical Sciences, Ubon Ratchathani University, Ubon Ratchathani 34190, Thailand
* Correspondence: opanasopit_p@su.ac.th (P.O.); worranan.r@ubu.ac.th (W.R.)

Abstract

Boesenbergia rotunda (L.) Mansf. contains pinostrobin and panduratin A, which are poorly water-soluble compounds with limited passive skin permeation. This study investigated the potential of microspicules (MSs) and microneedles (MNs) for transdermal delivery of a *B. rotunda*-loaded microemulsion (B-ME) formulation. The *B. rotunda* extract was incorporated into an ME and then loaded into MS gel and MN patch formulations. Physicochemical properties and transdermal performance were evaluated. A 5% (*w*/*w*) *B. rotunda* extract-loaded ME exhibited a nanometer-sized droplet diameter (165.4 nm), high incorporation efficiencies of pinostrobin (74.67%) and panduratin A (62.98%), and successful incorporation into both MS gel and MN patch. Microscopic images showed microneedling shapes of MSs with spicules extending from opposite ends, with a middle width of 17.00 µm and a spicule length of 239.00 µm, and sharply conical-shaped MN tips arranged in a 13 × 13 array (169 needles), with a height of 646.06 µm and a base width of 574.29 µm. The B-ME-loaded MN patch significantly enhanced skin permeation and deposition of both pinostrobin and panduratin A compared with the B-ME-loaded MS gel and B-ME ($p < 0.05$). The B-ME-loaded MN patch increased the flux of pinostrobin and panduratin A by 4.08-fold, respectively, compared with B-ME, whereas the B-ME-loaded MS gel increased the corresponding fluxes by 2.00-fold and 9.68-fold. In conclusion, the MN patch demonstrated strong potential as a transdermal delivery system for B-ME, indicating a synergistic effect between the nanoscale microemulsion carrier and microscale needle-assisted skin delivery, thereby improving the delivery efficiency of hydrophobic compounds from *B. rotunda* extract.

Keywords: *Boesenbergia rotunda*; microemulsion; microneedles; microspicules; skin permeation

Check for updates

Academic Editor: Natasa Skalko-Basnet

Received: 9 October 2026
Revised: 19 November 2026
Accepted: 25 November 2026
Published: 28 November 2026

Copyright: © 2026 by the authors. Published by MDPI on behalf of the Österreichische Pharmazeutische Gesellschaft. Licensee MDPI, Basel, Switzerland. This article is an open access article distributed under the terms and conditions of the Creative Commons Attribution (CC BY) license.

1. Introduction

Boesenbergia rotunda (L.) Mansf., commonly referred to as fingerroot and belonging to the family Zingiberaceae, is a well-recognized medicinal plant widely used in traditional

Southeast Asian medicine. The rhizome of *B. rotunda* is rich in bioactive phytochemicals, including pinostrobin, cardamonin, boesenbergin, 5,7-dihydroxyflavone, 1,8-cineole, and panduratin A [1]. Among these constituents, panduratin A has attracted considerable attention because of its antiadipogenic and lipolytic activities. Topical formulations containing panduratin A have demonstrated potential for lipolytic body products by promoting subcutaneous fat reduction [2]. Likewise, *B. rotunda* extract containing pinostrobin and panduratin A has been reported to inhibit adipogenesis and exhibit body-firming effects [3]. However, the therapeutic application of pinostrobin and panduratin A is limited by their poor aqueous solubility, low skin permeability, and susceptibility to environmental factors such as elevated temperature, light exposure, pH fluctuations, and enzymatic degradation [4]. Moreover, transdermal drug absorption is inherently challenging because the stratum corneum acts as the primary barrier to the penetration of exogenous substances [5]. Thus, transdermal drug delivery systems have been developed to modify or breach the stratum corneum, leading to enhanced drug permeation through the skin [6].

Effective nanocarrier systems for *B. rotunda* extract have been developed, with microemulsions (MEs) being reported to enhance the solubility, permeability, and overall therapeutic efficacy of its poorly water-soluble bioactive constituents [7]. Nevertheless, passive permeation enhancement approaches alone remain insufficient to fully overcome the formidable skin barrier. In this context, the integration of nanocarrier systems with microneedle technology has emerged as an efficient physical enhancement strategy, enabling the bypass of the stratum corneum barrier and facilitating effective transdermal delivery of active compounds [8].

Dissolving microneedles (MNs) are minimally invasive delivery systems that enhance transdermal drug delivery by penetrating the stratum corneum, creating transient microchannels, and dissolving within the skin to enable localized and controlled drug release [9]. Their combination with MEs offers a synergistic approach that integrates both chemical and physical permeation-enhancement mechanisms. Previous studies have shown that ME-loaded MNs significantly improve drug permeation, achieving nearly threefold higher delivery compared to ME alone, while also enhancing therapeutic outcomes [10]. Similarly, MNs incorporating a progesterone-loaded self-microemulsifying drug delivery system (SMEDDS) improved permeation and sustained release. These findings support the potential of combining ME-based nanocarriers with MN technology for efficient transdermal drug delivery [11].

Apart from MN patches, microspicules (MSs) have recently emerged as a promising physical penetration-enhancement technology for transdermal drug delivery. MSs are needle-like structures of sponge spicules with tips growing out from two opposite sites [12,13]. Upon massaging *Spongillia* spicules onto the skin, mechanical separation of the epidermal layers has been reported, leading to reduced keratinocyte cohesion, increased stratum corneum sloughing, and removal of loosened keratinocytes [14]. In a previous study, panduratin A isolated from *B. rotunda* and incorporated into a topical MS serum might have enhanced subcutaneous adipose tissue delivery, demonstrating its potential for use in a lipolytic body product [2].

However, the comparative transdermal delivery performance of MSs and MNs when combined with a B-ME remains unclear, particularly in terms of the skin permeation and deposition of pinostrobin and panduratin A. Therefore, this study aimed to investigate the effect of MSs and MNs as potential transdermal delivery systems for a *B. rotunda*-loaded microemulsion (B-ME). The *B. rotunda* extract was prepared as an ME formulation and then loaded into an MS gel and MN patch. The physicochemical characteristics of the developed formulations and their ex vivo skin permeation and deposition were investigated.

2. Materials and Methods

2.1. Materials

The ethanolic extract of *B. rotunda* rhizomes was obtained from the Faculty of Pharmaceutical Sciences, Ubon Ratchathani University, Thailand [2]. Quantitative analysis by HPLC revealed pinostrobin and panduratin A contents as 181.02 ± 2.73 mg/g and 80.90 ± 1.05 mg/g of the crude extract, respectively.

Pinostrobin standard and d-limonene were purchased from Sigma-Aldrich Co. (St. Louis, MO, USA). Panduratin A was purchased from phyproof® Reference Substance (PhytoLab GmbH & Co., Vestenbergsgreuth, Germany). Caprylocaproyl polyoxyl-8 glycerides (Labrasol®) was kindly provided by Gattefossé (Paramus, NJ, USA). Diethylene glycol monoethyl ether (Transcutol® CG) and polyacrylate crosspolymer-6 (Sepimax™ ZEN) were purchased from Chanjao Longevity Co., Ltd. (Bangkok, Thailand). Polyvinylpyrrolidone (PVP), polyvinyl alcohol (PVA), glycerin, Phenoxyethanol (and) Chlorphenesin (and) Glycerin (Microcare® PHC), and disodium ethylenediaminetetraacetate (EDTA) were purchased from Krungthepchemi Co., Ltd. (Bangkok, Thailand). Sponge spicule extract powder (MS; ≥98% spicules) was obtained from Hunan Sunshine Bio-Tech Co., Ltd. (Changsha, China). Acetonitrile was obtained from Fisher Scientific (Seoul, Republic of Korea). Orthophosphoric acid, absolute ethanol (99.9%), and methanol were acquired from Merck & Co. (Darmstadt, Germany). Absolute ethanol was kept tightly sealed and opened only when needed during sample preparation to minimize moisture absorption. All other chemicals and solvents were of analytical reagent grade.

2.2. Preparation of B. rotunda Extract-Loaded Microemulsion

B. rotunda extract (5% *w*/*w*) was incorporated into the ME system according to a previous study [7]. Briefly, the ME vehicle consisted of 63.34% Labrasol® and Transcutol® CG (3:1), 18.33% d-limonene, and 18.33% water. The B-ME was prepared to contain 5% (*w*/*w*) *B. rotunda* crude extract and 95% (*w*/*w*) of the ME vehicle. The formulation was stirred for 10 min to achieve homogeneous mixing. Only clear and homogeneous formulations without visible precipitation of the crude extract were collected.

The droplet size, PDI, and zeta potential of the ME formulations were determined using photon correlation spectroscopy (PCS) with a Zetasizer Nano Series analyzer (Malvern Instruments, Malvern, UK). The incorporation of pinostrobin and panduratin A from *B. rotunda* extract-loaded ME was diluted with absolute ethanol and centrifuged at 10,000 rpm for 10 min. The supernatant was filtered through a 0.45 µm nylon membrane filter and analyzed using HPLC. The incorporation efficiency was calculated according to Equation (1):

$$\% \text{ Incorporation efficiency} = \frac{\text{Concentration of Pinostrobin or Panduratin A in the formulation}}{\text{Initial concentration of Pinostrobin or Panduratin A added}} \times 100 \quad (1)$$

2.3. Preparation of Microspicule Gel Loading B-ME

The B-ME-loaded MS gel was prepared according to the composition shown in Table 1. Briefly, 5% (*w*/*w*) *B. rotunda* crude extract was dissolved in the ME vehicle and then incorporated into the gel base. The gel base consisted of distilled water, glycerin, polyacrylate crosspolymer-6, Microcare® PHC, and disodium EDTA. After homogeneous mixing, 0.5% (*w*/*w*) MS was incorporated into the formulation. The physical properties of the formulation were evaluated, such as appearance, pinostrobin and panduratin A content, and MS shape using a microscope (Nikon DS-Ri2, Nikon Corporation, Tokyo, Japan).

Table 1. Composition of B-ME-loaded MS gel formulation.

Ingredients	Concentration (%*w*/*w*)
B. rotunda crude extract	5.00
Microemulsion	30.00
Polyacrylate crosspolymer-6	0.54
Disodium EDTA	0.05
Glycerin	4.00
Phenoxyethanol (and) Chlorphenesin (and) Glycerin	0.80
Microspicules	0.50
Distilled water	q.s. to 100

2.4. Preparation of Microneedle Patch Loading B-ME

MN patches were fabricated using 40% (*w*/*w*) PVP and 20% (*w*/*w*) PVA stock solutions, which were mixed at a weight ratio of 1:4 (PVP solution:PVA solution) to prepare the polymer mixture. Subsequently, a B-ME containing 5% (*w*/*w*) *B. rotunda* crude extract was incorporated into the stock polymer mixture under continuous stirring to obtain a homogeneous casting solution. The final casting solution consisted of 20% (*w*/*w*) B-ME and 80% (*w*/*w*) polymer mixture, corresponding to a nominal crude extract concentration of 1% (*w*/*w*).

The MN arrays were prepared using a micromolding technique. Briefly, the formulation was accurately weighed and cast into laser-engineered silicone micromold templates. The molds were centrifuged at 4000 rpm for 30 min to ensure complete filling of the needle cavities and formation of well-defined needle tips. The molds were then dried at room temperature for 48 h to allow solvent evaporation and solidification of the polymer matrix. After drying, the MN arrays were carefully demolded and stored in a desiccator until further evaluation.

The physicochemical properties of the MN patches were characterized, including visual appearance and morphological features, using a Dino-Lite Edge 5MP digital microscope (Dino-Lite AM7915 series, Hsinchu, Taiwan). Functional performance was further assessed in terms of skin insertion capability, dissolution time, and quantitative determination of pinostrobin and panduratin A content by HPLC.

2.5. HPLC Analysis

Ethanolic samples of *B. rotunda* were analyzed using a Thermo Scientific™ Dionex™ UltiMate 3000 HPLC system (Dionex Softron GmbH, Germering, Germany) with a photodiode array detector and a C18 column (VertiSep™ GES, 4.6 × 250 mm, 5 µm; Vertical Chromatography Co., Ltd., Bangkok, Thailand). The mobile phase consisted of acetonitrile and 0.1% phosphoric acid, employing a linear gradient from 50% to 100% acetonitrile over 5 min, held for 10 min, and returned to 50% over the next 10 min (total runtime: 25 min). Detection was at 285 nm. The injection volume and flow rate were 10 µL and 1.0 mL/min, respectively. Method validation included assessments of specificity, linearity, detection and quantification limits, precision, and accuracy (details in Supplementary Data).

2.6. Ex Vivo Skin Permeation and Deposition Study

Fresh abdominal skin was excised from intrapartum stillborn piglets obtained from a local farm in Ubon Ratchathani Province, Thailand. Skin collection was approved by the Animal Experimentation Ethics Committee, Ubon Ratchathani University, Ubon Ratchathani, Thailand (Approval No. 27/2568/IACUC). After excision, the underlying adipose tissue was carefully removed using surgical scissors to obtain skin specimens with a thickness of approximately 600–700 µm. The prepared skin was stored at −20 °C until use.

The ex vivo skin permeation study and skin deposition studies were conducted based on the method reported previously [7], with minor modifications. Briefly, abdominal porcine skin was mounted on vertical Franz-type diffusion cells with an effective diffusion area of 2.01 cm^2 and a receptor-compartment volume of 6 mL. For the B-ME and B-ME-loaded MS gel groups, 2 mL of each formulation was applied to the donor compartment. For the B-ME-loaded MS gel group, 2 mL of the formulation was applied to the skin surface and gently massaged for 2 min using a forefinger covered with a medical glove, according to the previously reported application method [2]. For the B-ME-loaded MN group, one MN patch was applied to the skin under a constant force of 10 N for 2 min before the experiment. The receptor medium consisted of PBS (pH 7.4) containing polysorbate 20 (5 g/L) mixed with ethanol at a 1:1 (*v*/*v*) ratio and was maintained at 32 ± 0.5 °C under continuous magnetic stirring. Receptor medium (0.5 mL) was collected at predetermined intervals (1, 2, 4, 6, 8, and 24 h) and immediately replaced with an equal volume of fresh medium. The collected samples were analyzed by HPLC.

After 24 h, the skin surface was rinsed with distilled water to remove residual formulation and gently blotted dry with tissue paper before extraction of the skin samples. The skin samples were then cut into small pieces and extracted with 2 mL of ethanol in an ultrasonic bath for 30 min. The concentrations of pinostrobin and panduratin A in the extracts were determined by HPLC.

The comparison of skin permeation and deposition among dosage forms with different drug-loading capacities was based on the percentage of the initial amount of each compound applied in the respective formulation, as calculated using Equations (2) and (3):

$$\%\text{Cumulative permeation} = \frac{\text{cumulative pinostrobin or panduratin A permeated at time}}{\text{initial pinostrobin or panduratin A applied}} \times 100 \quad (2)$$

$$\%\text{Skin deposition} = \frac{\text{Amount of pinostrobin or panduratin A deposited into the skin}}{\text{initial pinostrobin or panduratin A applied}} \times 100 \quad (3)$$

The cumulative amount of drug permeation per unit diffusion area (Q/A, μg/cm^2) was calculated at each sampling time. The permeation flux (μg/cm^2/h) was determined from the slope of the linear region of the cumulative amount permeated per unit area versus time profile using linear regression. For pinostrobin, the regression intervals were 4–24 h for the B-ME and B-ME-loaded MS gel and 1–8 h for the B-ME-loaded MN patch. For panduratin A, the corresponding intervals were 1–8 h, 1–4 h, and 1–8 h, respectively. The linear region was selected from the portion of each permeation profile showing an approximately linear increase in cumulative permeation. The coefficient of determination (R^2) values ranged from 0.8969 to 0.9952 for pinostrobin and from 0.9073 to 0.9871 for panduratin A. The permeability coefficient (K_P, cm/h) and the enhancement ratio (ER) were calculated using Equations (4) and (5), respectively.

$$K_P = J/C_0 \quad (4)$$

where J is the flux (μg/cm^2/h), and C_0 is the initial concentration of the active compound in the donor formulation (μg/cm^3).

$$ER = J_{test}/J_{B\text{-}ME} \quad (5)$$

where J_{test} and $J_{B\text{-}ME}$ represent the mean steady-state fluxes of the test formulation and B-ME reference formulation, respectively.

2.7. Statistical Analysis

Results are expressed as mean ± standard deviation (SD). The homogeneity of variance was assessed using Levene's test. One-way ANOVA was used for comparisons among

formulations. Tukey's HSD post hoc test was applied when the assumption of homogeneity of variance was met, whereas the Games–Howell post hoc test was used when variances were not homogeneous. A $p < 0.05$ was considered statistically significant.

3. Results

3.1. Physicochemical Properties of B-ME

The B-ME formulation appeared as a clear yellow solution. The mean particle diameter was 165.4 nm, with a narrow size distribution (PDI ≈ 0.26), indicating good homogeneity of the nanoparticle system. The zeta potential was approximately 0.17 mV, reflecting a near-neutral surface charge. Quantitative analysis demonstrated that the B-ME contained 9.71 ± 0.84 mg/mL of pinostrobin and 3.95 ± 0.29 mg/mL of panduratin A. The formulation was prepared using 5% (*w*/*w*) *B. rotunda* extract, for which the percent incorporation efficiencies were 74.67 ± 4.75% for pinostrobin and 62.98 ± 3.72% for panduratin A. These values indicate highly efficient incorporation of both bioactive compounds into the microemulsion system, due to the strong solubilization capacity of the ME system and its suitability as a carrier for hydrophobic constituents of *B. rotunda* extract.

3.2. Physicochemical Properties of Microspicule Gel Loading B-ME

The B-ME was completely mixed with the MS gel, in which microneedling shapes of MSs were a tip growing out from two opposite sites with a 17.00 ± 2.65 µm middle width and 239.00 ± 22.52 µm spicule length (Figure 1a). The formulation exhibited a good appearance and smooth texture upon application onto the skin. Pinostrobin and panduratin A contents were 11.07 ± 2.0 mg/mL and 3.55 ± 0.67 mg/mL, respectively.

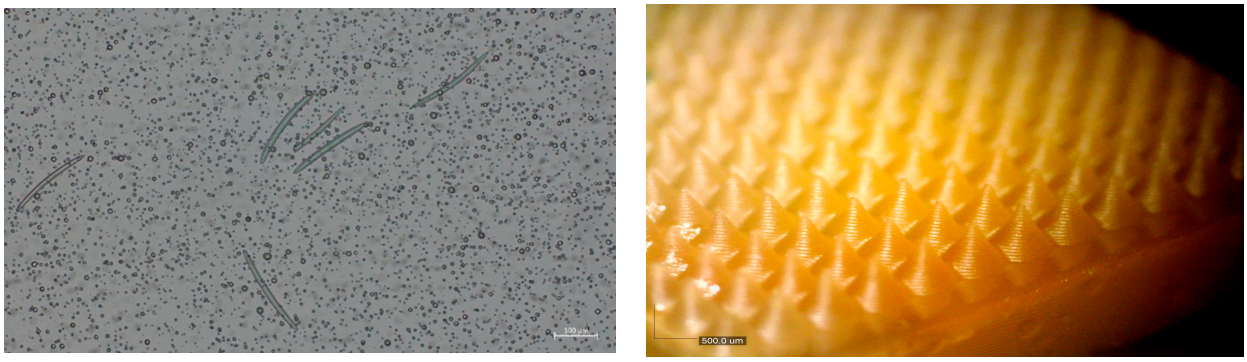

(**a**) (**b**)

Figure 1. Microscopic images of the B-ME-loaded MS gel (**a**) and MN patch (**b**).

3.3. Physicochemical Properties of MN Patch Loading B-ME

The B-ME-loaded MN was successfully incorporated into the MN patch. Digital microscopy (Figure 1b) revealed the distinctive physical appearance of the PVP and PVA MNs, displaying sharply conical-shaped needle tips (13 × 13 needles; 169 arrays) with a height of 646.06 ± 0.09 µm and a base width of 574.29 ± 0.13 µm. The pinostrobin and panduratin A contents in the MN patch were 189.32 ± 5.04 µg and 53.91 ± 2.59 µg per patch, respectively. The MN array in the skin was completely dissolved within 1 h, and the skin insertion was complete at 80.47–100% insertion. These findings underscore the suitability of the MN patch for loading the B-ME as a transdermal delivery system for pinostrobin and panduratin A from *B. rotunda* extract.

3.4. Skin Permeation and Deposition

The cumulative permeation profiles of pinostrobin and panduratin A across porcine skin are presented in Figure 2. The incorporation of the B-ME into dissolving MN patches markedly enhanced transdermal delivery compared with the B-ME and B-ME-loaded MS gel throughout the 24 h study period. For pinostrobin (Figure 2a), no detectable permeation was observed from the B-ME and MS gel during the initial 4 h. Detectable permeation from the MS gel was first observed at 6 h and gradually increased to 0.130 ± 0.110% at 24 h, whereas the B-ME exhibited limited permeation throughout the 24 h study period and reached a cumulative permeation of only 0.034 ± 0.018%. In contrast, the MN patch demonstrated rapid and sustained permeation across the skin and achieved the highest cumulative permeation at 24 h (1.162 ± 0.419%), which was significantly greater than that of the B-ME and MS gel ($p < 0.05$).

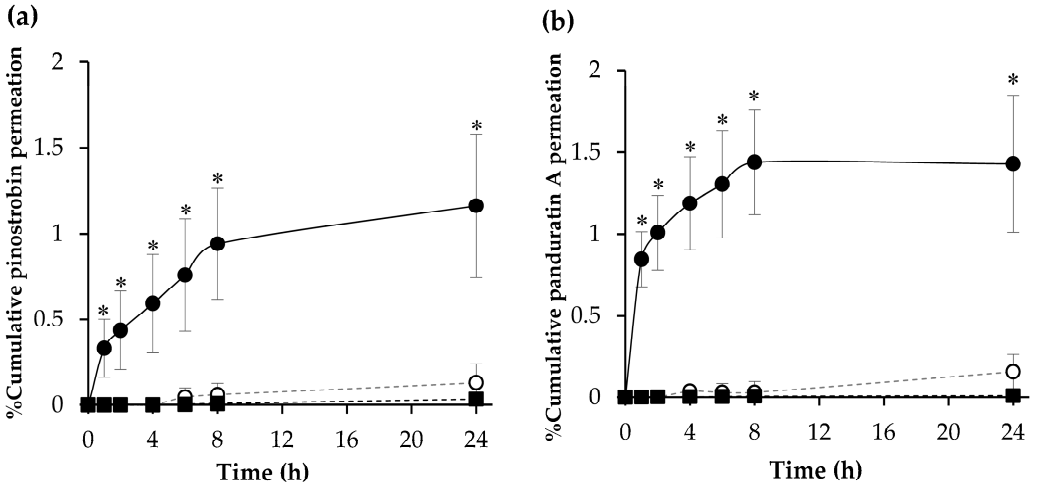

Figure 2. Percent cumulative permeation vs. time profile of (**a**) pinostrobin and (**b**) panduratin A from B-ME (■), B-ME-loaded MS gel (○), and B-ME-loaded MN patch (●) after 24 h of skin permeation. * indicates a significant difference compared with B-ME at the corresponding time point ($p < 0.05$).

A similar permeation pattern was observed for panduratin A (Figure 2b). The B-ME exhibited negligible transdermal permeation throughout the study period and reached a cumulative permeation of only 0.003 ± 0.001% at 24 h. Although incorporation into the MS gel resulted in a slight increase in transdermal delivery, percent cumulative permeation remained limited (0.253 ± 0.324%). In comparison, loading into the MN patch substantially improved panduratin A delivery, exhibiting the highest percent cumulative permeation at 24 h (1.429 ± 0.025%), which was significantly higher than that from the B-ME and MS gel ($p < 0.05$).

The penetration parameters calculated from the cumulative permeation profiles are summarized in Table 2. For pinostrobin, the B-ME-loaded MN patch exhibited the highest flux, followed by the B-ME-loaded MS gel and B-ME alone. The flux and permeability coefficient (K_p) of pinostrobin delivered from the MN patch were significantly higher than those of the B-ME ($p < 0.05$), whereas the B-ME-loaded MS gel showed no significant difference compared with the B-ME ($p > 0.05$). The ER of the B-ME-loaded MN patch was 4.08-fold, which was substantially greater than that of the B-ME-loaded MS gel (2.00-fold), indicating that the MN patch was more effective in enhancing the transdermal permeation of pinostrobin.

Table 2. The penetration parameters of pinostrobin and panduratin A from B-ME formulations.

Formulations	Flux ($\mu g/cm^2/h$)	K_p (cm/h) ($\times 10^{-3}$)	ER
	Pinostrobin		
B-ME	0.1595 ± 0.0226	0.0082 ± 0.0053	-
B-ME-loaded MS gel	0.3188 ± 0.1854	0.0137 ± 0.0080	2.00
B-ME-loaded MN patch	0.6512 ± 0.1678 *	3.4152 ± 0.8798 *	4.08
	Panduratin A		
B-ME	0.0069 ± 0.0012	0.0009 ± 0.0002	-
B-ME-loaded MS gel	0.0671 ± 0.0616	0.0085 ± 0.0078	9.68
B-ME-loaded MN patch	0.1758 ± 0.0224 *	3.2421 ± 0.4137 *	25.35

Note: Flux and K_p are presented as mean ± SD ($n = 3$). * indicates a significant difference from B-ME ($p < 0.05$).

For panduratin A, the B-ME-loaded MN patch also exhibited significantly higher flux and K_p values than both B-ME and the B-ME-loaded MS gel ($p < 0.05$). The ER achieved with the B-ME-loaded MN patch was 25.35-fold, which was substantially greater than that of the B-ME-loaded MS gel (9.68-fold). These findings demonstrate that incorporation of the B-ME into dissolving MN patches significantly enhanced the transdermal permeation of both pinostrobin and panduratin A compared with B-ME alone and the B-ME-loaded MS gel.

Supporting the skin permeation findings, skin deposition after 24 h is presented in Figure 3. The B-ME-loaded MN patch showed significantly higher deposition of both pinostrobin and panduratin A than the B-ME and B-ME-loaded MS gel ($p < 0.05$). Pinostrobin deposition increased from 0.225 ± 0.109% and 0.376 ± 0.245% in the B-ME and MS gel to 2.133 ± 0.720% in the MN patch, while panduratin A deposition increased from 0.093 ± 0.052% and 0.286 ± 0.237% to 1.245 ± 0.184%, respectively. These results demonstrate the superior ability of the MN patch to enhance the deposition of both bioactive compounds within the skin.

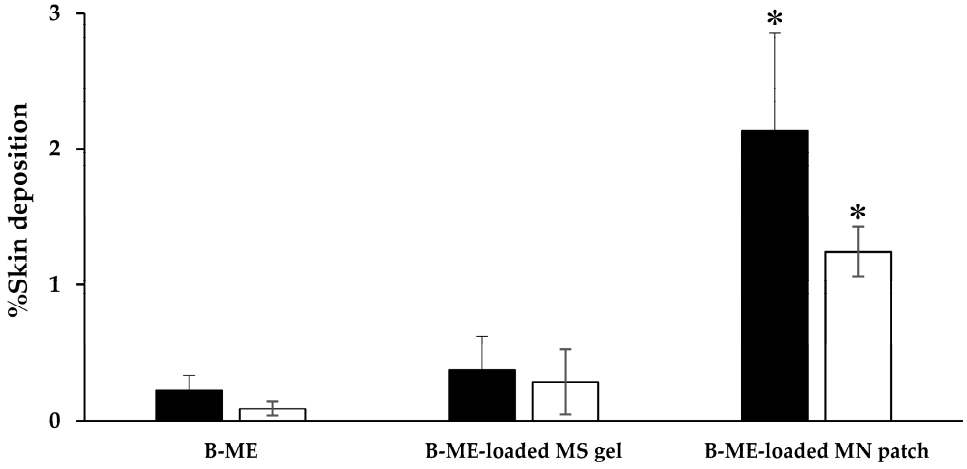

Figure 3. Skin deposition of pinostrobin (■) and panduratin A (□) from B-ME, B-ME-loaded MS gel, and B-ME-loaded MN patch after 24 h of skin permeation. * indicates a significant difference from B-ME ($p < 0.05$).

4. Discussion

B. rotunda ethanolic extract contains the major bioactive compounds pinostrobin and panduratin A (Figures S2 and S3), both of which exhibit poor aqueous solubility and limited skin permeability because of their hydrophobic nature [7]. Passive transdermal delivery of these phytochemicals is restricted by the barrier function of the stratum corneum, resulting

in limited drug penetration into deeper skin layers [15]. Incorporation of the extract into an ME system improved the solubilization and thermodynamic activity of these hydrophobic compounds, thereby facilitating their partitioning into the skin. A previous study reported that an optimized ME formulation composed of Labrasol®, Transcutol®, d-limonene, and water exhibited a nanosized droplet diameter and high entrapment efficiency for pinostrobin derived from *B. rotunda* extract [7].

The penetration-enhancing effect of MEs is primarily attributed to their small droplet size and large surface area, which facilitates drug transport into and across the skin. The ability of MEs to increase the skin penetration of compounds can also be attributed to their individual components. Surfactants, oil phase, and other penetration enhancers incorporated in the system can diffuse to the skin surface and increase the permeation of drugs, either by disrupting the lipid structure of the stratum corneum (facilitating diffusion through the skin barrier) or by increasing the solubility of the drug in the skin (i.e., increasing the partition coefficient of the drug between the skin and the vehicle) [16–18]. Labrasol® and Transcutol® were used as surfactant and co-surfactant in the ME system, and both have been reported to function as skin penetration enhancers. Transcutol® (diethylene glycol monoethyl ether) increases the penetration of drug molecules by a "pull" effect, which involves dragging the drug molecules while diffusing through the skin. A previous study reported that Transcutol® enhances the skin permeation of genistein by forming an intracutaneous depot, modifying the stratum corneum, and increasing drug solubility within the skin [19,20]. Similarly, penetration enhancer-containing particles incorporating Labrasol® (caprylocaproyl polyoxyl-8 glycerides) exhibited highly deformable and skin-permeable particles, facilitating passage through the stratum corneum by increasing membrane elasticity [21]. The lipophilicity of d-limonene also plays an important role in determining the penetration enhancement effect for lipophilic drugs. Terpenes with higher lipophilicity (higher log *p* values) interact more readily with the intercellular lipids of the stratum corneum, thereby fluidizing or perturbing the integrity of the skin barrier and facilitating drug transport across the skin [22,23].

Although the ME system improved the solubility and skin permeability of pinostrobin and panduratin A, their permeation across intact skin remained limited because the stratum corneum constitutes the principal barrier to passive transdermal transport [15]. In our previous study [7], the optimized ME containing Labrasol® and Transcutol® enhanced the skin permeation and deposition of pinostrobin compared with an oil-based formulation, in which no detectable permeation of pinostrobin was observed. However, despite the penetration-enhancing properties of these excipients, they do not completely overcome the barrier function of the stratum corneum. The relatively low cumulative permeation observed with the B-ME in the present study, particularly compared with the MS gel and MN patch, may be attributed to the limitations of passive skin permeation rather than a lack of penetration-enhancing activity of the ME components. The B-ME-loaded MS gel showed greater skin delivery than B-ME alone. Sponge spicules are naturally derived needle-like silica structures that have been reported to generate microchannels within the superficial layers of the skin during topical massage, reducing the barrier function of the stratum corneum by disrupting keratinocyte cohesion and promoting superficial desquamation, thereby facilitating the penetration of active compounds [12,24,25]. Previous studies have shown that panduratin A isolated from *B. rotunda* and incorporated into a topical MS serum exhibited greater skin permeability than the corresponding serum without MSs, supporting the potential role of MSs in enhancing skin penetration [2].

In contrast, the enhanced permeation observed with the MN patch may be associated with the distinct mechanism by which a dissolving MN interacts with the skin barrier. Unlike MSs, which are applied by topical massage, the MNs were arranged in a defined array and

inserted into the skin under a controlled application force. In the MN formulation, the B-ME served primarily as a solubilization system for the poorly water-soluble pinostrobin and panduratin A before incorporation into the PVP/PVA matrix. Following insertion, dissolution of the polymeric needle ma trix released the incorporated compounds at the sites of microchannel formation, thereby providing a different pathway for transdermal delivery [26,27]. Thus, the greater permeation observed with the MN formulation may reflect differences in the mode and extent of barrier disruption and subsequent drug release rather than needle dimensions alone.

The enhanced performance of the MN patch may also be attributed to the physicochemical properties of the dissolving PVP/PVA polymer matrix. Previous studies have reported that PVP alone possesses relatively limited mechanical strength for effective skin insertion [28]. Blending PVP with PVA improves the mechanical properties of dissolving MNs through intermolecular hydrogen bonding between the hydroxyl groups of PVA and the carbonyl groups of PVP, resulting in a stronger and more stable polymer network [29]. Due to its high hydrophilicity and excellent water solubility, PVP readily absorbs interstitial fluid and rapidly dissolves after skin insertion, leading to the release of the incorporated pinostrobin and panduratin A [30,31]. Meanwhile, PVA serves as the structural component of the MNs, providing sufficient mechanical strength and flexibility to withstand the insertion force while maintaining needle integrity during insertion [29,32,33]. The combined properties of PVP and PVA enable efficient skin insertion followed by rapid matrix dissolution, thereby allowing localized release of the incorporated compounds and enhancing the skin permeation and deposition of pinostrobin and panduratin A compared with B-ME alone and the B-ME-loaded MS gel. The nanoscale structure of the B-ME after incorporation into the PVP/PVA matrix and subsequent MN dissolution was not characterized in this study; therefore, preservation of the original ME droplet structure cannot be confirmed.

Differences in drug loading, applied dose, and formulation composition should be considered when interpreting the permeation results. In this study, the ME was used primarily to solubilize pinostrobin and panduratin A, while the amount of B-ME incorporated into the MN matrix was limited by the need to maintain adequate mechanical properties for skin insertion. Preliminary formulation trials identified 20% (*w*/*w*) B-ME as the highest feasible loading level that maintained acceptable MN properties. Despite its lower drug content, the MN patch showed a higher percentage of cumulative permeation relative to the initial applied dose than the B-ME and MS gel formulations, indicating delivery of a greater fraction of its incorporated compounds. However, differences in formulation composition and applied dose limit direct comparisons of delivery efficiency among the three systems. Further studies using dose-matched formulations are needed to clarify the contribution of each delivery mechanism.

The relatively low amount of panduratin A detected in the receptor medium compared with pinostrobin may be attributed to differences in their initial contents and physicochemical properties. The *B. rotunda* extract contained less panduratin A (80.90 ± 1.05 mg/g) than pinostrobin (181.02 ± 2.73 mg/g), resulting in a lower initial amount of panduratin A in the developed formulations. Pinostrobin has been identified as a chemical marker of *B. rotunda* [34], consistent with its relatively high abundance among the flavonoids reported in fingerroot [35,36]. Furthermore, panduratin A has a higher molecular weight (406.51 g/mol) and greater lipophilicity (WLogP = 6.01) than pinostrobin (270.28 g/mol; WLogP = 2.78), which may influence its diffusion and partitioning across the skin [37]. Its greater lipophilicity may also favor retention within the skin rather than permeation into the receptor medium [38,39]. Therefore, the low amounts of panduratin A detected in the receptor medium may limit the accuracy of quantitative permeation estimates. Con-

sequently, these results should be interpreted cautiously as reflecting general permeation trends rather than precise quantitative estimates of panduratin A permeation.

The limited drug-loading capacity of dissolving MN remains an important consideration because of the small volume available within the needle matrix. In the present study, each B-ME-MN patch contained 190.69 μg of pinostrobin and 54.21 μg of panduratin A. Although the MN patch significantly enhanced the ex vivo skin permeation and deposition of both compounds compared with B-ME alone and the B-ME-loaded MS gel, therapeutic efficacy was not evaluated. Therefore, whether the delivered amounts are sufficient to produce the intended biological or therapeutic effects remains to be established. Further in vivo and clinical studies, including dose–response evaluation, are required to establish an effective dose and confirm the efficacy and safety of the developed MN delivery system.

5. Conclusions

This study demonstrated that incorporation of a B-ME into dissolving MN patches significantly enhanced transdermal delivery compared with B-ME alone and a B-ME-loaded MS gel. The MN patch achieved significantly higher percentages of skin permeation and skin deposition of both pinostrobin and panduratin A relative to the initial applied dose, indicating improved transdermal delivery of a greater fraction of the active compounds. Although differences in formulation composition and applied dose limit direct comparisons of the individual penetration-enhancement mechanisms, these findings provide comparative evidence of the delivery performance of the developed formulations. Therefore, the B-ME-loaded MN patch may represent a promising formulation approach for enhancing the skin delivery of pinostrobin and panduratin A.

Supplementary Materials: The following supporting information can be downloaded at https://www.mdpi.com/article/10.3390/scipharm94040120/s1, Figure S1: The UV spectra of standard pinostrobin and panduratin A recorded from the standard and *B. rotunda* extract; Figure S2: HPLC chromatograms of (a) pinostrobin (25 μg/mL) and panduratin A (25 μg/mL) standards, (b) *B. rotunda* extract (0.2 mg/mL), and (c) spike *B. rotunda* (0.2 mg/mL) with standard pinostrobin (25 μg/mL) and panduratin A (25 μg/mL); Figure S3: Chemical structures of (a) pinostrobin and (b) panduratin A; Table S1: Linear range, regression equation, coefficient of determination (R^2), LOD, and LOQ of calibration curves of pinostrobin and panduratin A; Table S2: %Recovery of pinostrobin and panduratin A in *B. rotunda* extract; Table S3: Intra-day and inter-day precision of pinostrobin and panduratin A; Table S4: Intra-day and inter-day precision of *B. rotunda* extract.

Author Contributions: Conceptualization, P.W. and W.R.; methodology, P.W., K.J., C.T., P.S. (Phaijit Sritananuwat), P.S. (Phuvamin Suriyaaumporn) and W.R.; visualization, P.W. and W.R.; writing—original draft preparation, P.W.; writing—review and editing, W.R. and P.O.; supervision, P.O.; funding acquisition, W.R. and P.O. All authors have read and agreed to the published version of the manuscript.

Funding: The authors would like to thank the Faculty of Pharmaceutical Sciences (Grant No. 0604.11-1/2568), Ubon Ratchathani University, and the Research and Creative Fund, Faculty of Pharmacy, Silpakorn University, for their financial support.

Institutional Review Board Statement: The animal study protocol was approved by the Animal Experimentation Ethics Committee of Ubon Ratchathani University, Ubon Ratchathani, Thailand (Approval No. 27/2568/IACUC; date of approval: 23 June 2025).

Informed Consent Statement: Not applicable.

Data Availability Statement: The data that support the findings of this study are available from the corresponding authors upon reasonable request.

Acknowledgments: The authors gratefully acknowledge the research facility support provided by the Faculty of Pharmacy, Silpakorn University. We also thank Wannaporn Phromyothin and Nutnicha Chaiyakham as the research assistants.

Conflicts of Interest: The authors declare no conflict of interest.

Abbreviations

The following abbreviations are used in this manuscript:

B-ME	*Boesenbergia rotunda* extract-loaded microemulsion
MN	Microneedle
MS	Microspicule
PVA	Polyvinyl alcohol
PVP	Polyvinylpyrrolidone
PDI	Polydispersity index
HPLC	High-performance liquid chromatography
PBS	Phosphate-buffered saline
K_p	Permeability coefficient
ER	Enhancement ratio

References

1. Kim, M.S.; Pyun, H.B.; Hwang, J.K. Effects of orally administered fingerroot (*Boesenbergia pandurata*) extract on oxazolone-induced atopic dermatitis-like skin lesions in hairless mice. *Food Sci. Biotechnol.* **2013**, *22*, 257–264. [CrossRef]
2. Jitsaeng, K.; Duangjit, S.; Sritananuwat, P.; Tansathien, K.; Opanasopit, P.; Rangsimawong, W. Potential lipolytic effect of panduratin A-loaded microspicule serum as a transdermal delivery approach for subcutaneous fat reduction. *Biol. Pharm. Bull.* **2023**, *46*, 1761–1768. [CrossRef] [PubMed]
3. Sritananuwat, P.; Samseethong, T.; Jitsaeng, K.; Duangjit, S.; Opanasopit, P.; Rangsimawong, W. Effectiveness and safety of *Boesenbergia rotunda* extract on 3T3-L1 preadipocytes and its use in capsaicin-loaded body-firming formulation: In vitro biological study and in vivo human study. *Cosmetics* **2024**, *11*, 24. Correction in *Cosmetics* **2024**, *11*, 66. https://doi.org/10.3390/cosmetics11030066. [CrossRef]
4. Suphakijudomkarn, P.; Suwanvecho, C.; Sithisarn, P.; Khemawoot, P.; Rojsanga, P. A stability-indicating HPLC method for determination of chemical markers in *Boesenbergia rotunda* extract capsules. *Pharm. Sci. Asia* **2025**, *52*, 55–64. [CrossRef]
5. Ramadon, D.; McCrudden, M.T.C.; Courtenay, A.J.; Donnelly, R.F. Enhancement strategies for transdermal drug delivery systems: Current trends and applications. *Drug Deliv. Transl. Res.* **2022**, *12*, 758–791. [CrossRef] [PubMed]
6. Singh, I.; Morris, A. Performance of transdermal therapeutic systems: Effects of biological factors. *Int. J. Pharm. Investig.* **2011**, *1*, 4–9. [CrossRef] [PubMed]
7. Wittayanukullack, P.; Opanasopit, P.; Suriyaamporn, P.; Rangsimawong, W. Formulation optimization and in vitro and ex vivo evaluation of *Boesenbergia rotunda* extract-loaded microemulsion using an experimental design model. *Pharm. Sci. Asia* **2025**, *52*, 506–517. [CrossRef]
8. Rangsimawong, W.; Duangjit, S.; Charoenputtakun, P.; Tansathien, K.; Ngawhirunpat, T.; Opanasopit, P. A dual approach using PEGylated nanocarriers and microneedles to enhance transdermal delivery of macromolecular proteins from goat placenta extract. *Pharmacia* **2025**, *72*, 1–11. [CrossRef]
9. Qu, F.; Geng, R.; Liu, Y.; Zhu, J. Advanced nanocarrier- and microneedle-based transdermal drug delivery strategies for skin diseases treatment. *Theranostics* **2022**, *12*, 3372. [CrossRef] [PubMed]
10. Li, J.; Tian, X.; Wang, K.; Jia, Y.; Ma, F. Transdermal delivery of celecoxib and α-linolenic acid from microemulsion-incorporated dissolving microneedles for enhanced osteoarthritis therapy. *J. Drug Target.* **2023**, *31*, 206–216. [CrossRef] [PubMed]
11. Suriyaamporn, P.; Aumklad, P.; Rojanarata, T.; Patrojanasophon, P.; Ngawhirunpat, T.; Pamornpathomkul, B.; Opanasopit, P. Fabrication of controlled-release polymeric microneedles containing progesterone-loaded self-microemulsions for transdermal delivery. *Pharm. Dev. Technol.* **2024**, *29*, 98–111. [CrossRef] [PubMed]
12. Villani, M. Use of Spongilla Spicules as a Dermabrasion Device or Resurfacing Modality. U.S. Patent Application US20100080853A1, 1 April 2010.
13. Kim, T.G.; Lee, Y.; Kim, M.S.; Lim, J. A novel dermal delivery system using natural spicules for cosmetics and therapeutics. *J. Cosmet. Dermatol.* **2022**, *21*, 4754–4764. [CrossRef] [PubMed]

14. Ha, J.M.; Lim, C.; Han, K.; Ha, J.C.; Lee, H.E.; Lee, Y.; Seo, Y.J.; Kim, C.D.; Lee, J.H.; Im, M. The effect of micro-spicule containing epidermal growth factor on periocular wrinkles. *Ann. Dermatol.* **2017**, *29*, 187–193. Correction in *Ann. Dermatol.* **2017**, *29*, 828. https://doi.org/10.5021/ad.2017.29.6.828. [CrossRef] [PubMed]
15. Alkilani, A.Z.; McCrudden, M.T.C.; Donnelly, R.F. Transdermal drug delivery: Innovative pharmaceutical developments based on disruption of the barrier properties of the stratum corneum. *Pharmaceutics* **2015**, *7*, 438–470. [CrossRef] [PubMed]
16. Kreilgaard, M. Influence of microemulsions on cutaneous drug delivery. *Adv. Drug Deliv. Rev.* **2002**, *54*, S77–S98. [CrossRef] [PubMed]
17. El Maghraby, G.M. Transdermal delivery of hydrocortisone from eucalyptus oil microemulsion: Effects of cosurfactants. *Int. J. Pharm.* **2008**, *355*, 285–292. [CrossRef] [PubMed]
18. Lopes, L.B. Overcoming the cutaneous barrier with microemulsions. *Pharmaceutics* **2014**, *6*, 52–77. [CrossRef] [PubMed]
19. Chadha, G.; Sathigari, S.; Parsons, D.L.; Babu, J. In vitro percutaneous absorption of genistein from topical gels through human skin. *Drug Dev. Ind. Pharm.* **2011**, *37*, 498–505. [CrossRef] [PubMed]
20. Virani, A.; Puri, V.; Mohd, H.; Michniak-Kohn, B. Effect of penetration enhancers on transdermal delivery of oxcarbazepine, an antiepileptic drug using microemulsions. *Pharmaceutics* **2023**, *15*, 183. [CrossRef] [PubMed]
21. Mura, S.; Manconi, M.; Fadda, A.M.; Sala, M.C.; Perricci, J.; Pini, E.; Sinico, C. Penetration enhancer-containing vesicles (PEVs) as carriers for cutaneous delivery of minoxidil: In vitro evaluation of drug permeation by infrared spectroscopy. *Pharm. Dev. Technol.* **2013**, *18*, 1339–1345. [CrossRef] [PubMed]
22. Yang, Z.; Teng, Y.; Wang, H.; Hou, H. Enhancement of skin permeation of bufalin by limonene via reservoir-type transdermal patch: Formulation design and biopharmaceutical evaluation. *Int. J. Pharm.* **2013**, *447*, 231–240. [CrossRef] [PubMed]
23. Chen, J.; Jiang, Q.D.; Chai, Y.P.; Zhang, H.; Peng, P.; Yang, X.X. Natural terpenes as penetration enhancers for transdermal drug delivery. *Molecules* **2016**, *21*, 1709. [CrossRef] [PubMed]
24. Zhang, S.; Ou, H.; Liu, C.; Zhang, Y.; Mitragotri, S.; Wang, D.; Chen, M. Skin delivery of hydrophilic biomacromolecules using marine sponge spicules. *Mol. Pharm.* **2017**, *14*, 3188–3200. [CrossRef] [PubMed]
25. Tansathien, K.; Chareanputtakhun, P.; Ngawhirunpat, T.; Opanasopit, P.; Rangsimawong, W. Hair growth promoting effect of bioactive extract from deer antler velvet-loaded niosomes and microspicules serum. *Int. J. Pharm.* **2021**, *597*, 120352. [CrossRef] [PubMed]
26. He, C.X.; He, Z.G.; Gao, J.Q. Microemulsions as drug delivery systems to improve the solubility and the bioavailability of poorly water-soluble drugs. *Expert Opin. Drug Deliv.* **2010**, *7*, 445–460. [CrossRef] [PubMed]
27. Zhang, Z.; Sun, Y.; Li, H.; Feng, J.; Cheng, M.; Tu, L. Enhancing transdermal drug delivery with dissolving microneedles: A review of optimization strategies and challenges. *J. Pharm. Sci.* **2026**, *115*, 104189. [CrossRef] [PubMed]
28. Teodorescu, M.; Bercea, M.; Morariu, S. Biomaterials of PVA and PVP in medical and pharmaceutical applications: Perspectives and challenges. *Biotechnol. Adv.* **2019**, *37*, 109–131. [CrossRef] [PubMed]
29. Jin, S.Y.; Park, E.J.-J.; Kwon, S.M.; Jung, H.S.; Kim, D.W. Rapidly dissolving microneedles incorporating lidocaine hydrochloride: A PVP/PVA-based approach for local anesthesia. *Pharmaceutics* **2025**, *17*, 1100. [CrossRef] [PubMed]
30. Dillon, C.; Hughes, H.; O'Reilly, N.J.; McLoughlin, P. Formulation and characterisation of dissolving microneedles for the transdermal delivery of therapeutic peptides. *Int. J. Pharm.* **2017**, *526*, 125–136. [CrossRef] [PubMed]
31. Shim, W.S.; Hwang, Y.M.; Park, S.G.; Lee, C.K.; Kang, N.G. Role of polyvinylpyrrolidone in dissolving microneedle for efficient transdermal drug delivery: In vitro and clinical studies. *Bull. Korean Chem. Soc.* **2018**, *39*, 789–793. [CrossRef]
32. Li, X.; Xiao, X.; Zhang, Y.; Long, R.; Lu, Q.; Zhang, H.; Wang, S. Microneedles based on hyaluronic acid-polyvinyl alcohol with antibacterial, anti-inflammatory, and antioxidant effects promote diabetic wound healing. *Int. J. Biol. Macromol.* **2024**, *282*, 137185. [CrossRef] [PubMed]
33. Lee, J.; Jeong, J.; Nguyen, V.P.; Hong, S.; Paulus, Y.M.; Lee, C.H. Microneedles for controlled and sustained intraocular drug delivery. *NPG Asia Mater.* **2025**, *17*, 33. [CrossRef] [PubMed]
34. Department of Medical Sciences, Ministry of Public Health. *Thai Herbal Pharmacopoeia 2021 (Supplementary 2022)*; Department of Medical Sciences, Ministry of Public Health: Nonthaburi, Thailand, 2022. Available online: https://bdn.dmsc.moph.go.th/th/detailAll/1083/ebook/136 (accessed on 19 November 2026).
35. Tan, B.C.; Tan, S.K.; Wong, S.M.; Ata, N.; Rahman, N.A.; Khalid, N. Distribution of flavonoids and cyclohexenyl chalcone derivatives in conventionally propagated and in vitro-derived field-grown *Boesenbergia rotunda* (L.) Mansf. *Evid. Based Complement. Alternat. Med.* **2015**, *2015*, 451870. [CrossRef] [PubMed]
36. Monton, C.; Kulvanich, P.; Chankana, N.; Rangsimawong, W.; Suksaeree, J.; Charoenchai, L.; Theanphong, O. Cluster analysis of fingerroot cultivated in different regions across Thailand and implementation of Quality by Design approach for R&D of fingerroot extract tablet. *Food Res. Int.* **2025**, *202*, 115728. [CrossRef] [PubMed]
37. Eiamart, W.; Wonganan, P.; Tadtong, S.; Samee, W. Panduratin A from *Boesenbergia rotunda* effectively inhibits EGFR/STAT3/Akt signaling pathways, inducing apoptosis in NSCLC cells with wild-type and T790M mutations in EGFR. *Int. J. Mol. Sci.* **2025**, *26*, 2350. [CrossRef] [PubMed]

38. Longgos, L.D.; Pequiro, E.B.; Liston, L.S.B.; Flores, K.A.M.; Ecoy, G.A.U.; Sakdiset, P.; See, G.L.L.; Arce, F.V., Jr. Effect of terpenes on the enhancement of skin permeation of lipophilic drugs: A systematic review. *Acta Med. Philipp.* **2024**, *58*, 59–71. [CrossRef] [PubMed]
39. Neubert, R.H.H. Mechanisms of penetration and diffusion of drugs and cosmetic actives across the human stratum corneum. *Eur. J. Pharm. Biopharm.* **2024**, *202*, 114394. [CrossRef] [PubMed]

Disclaimer/Publisher's Note: The statements, opinions and data contained in all publications are solely those of the individual author(s) and contributor(s) and not of MDPI and/or the editor(s). MDPI and/or the editor(s) disclaim responsibility for any injury to people or property resulting from any ideas, methods, instructions or products referred to in the content.